Protoplanetary Disks, Jets, and the Birth of the Stars

Guillem Anglada

Instituto de Astrofísica de Andalucía (CSIC), Glorieta de la Astronomía s/n, 18008 Granada, Spain

Abstract

Young stars are surrounded by rotating disks of gas and dust. These disks play an essential role in regulating the mass accretion onto the star and are the precursors of exoplanetary systems. Accretion disks also play an important role in driving the bipolar collimated ejections (jets) that remove the excess of angular momentum and allow the star to reach its final mass. Jets are partially ionized and their continuum free-free emission at centimeter wavelengths is a powerful tool to study at small scale (10-100 au) the region where they originate. Observations of the dust thermal emission at centimeter wavelengths are also well suited to study the distribution of dust grains that have evolved up to centimeter sizes and trace the signatures of planet formation in protoplanetary disks. I will present some recent results from VLA and ALMA observations of disks and jets in young stellar objects, and I will discuss future prospects with the SKA in this field.

1   Introduction

During the star-formation process a disk/jet system is originated. This system persists from the earliest protostellar stages until the end of accretion in the pre-main sequence phase, and plays a crucial role both in the formation of the star itself and in the development of a possible planetary system. The jet evacuates the excess of mass and angular momentum allowing the star to reach its final mass ([41]). The disk plays a fundamental role in the ejection of the jet ([34], [15]) but a still more important aspect is its potential to give rise to a planetary system as its final destination (see [24], [30]), [26]).

A combination of sensitive and high angular resolution observations in the centimeter and millimeter wavelength regimes using large radio interferometers, notably the upgraded Jansky Very Large Array (VLA) and the Atacama Large Millimeter/submillimeter Array (ALMA) are revealing with unprecedented detail the dust and ionized components of the disks

and jets associated with young stellar objects (YSOs). Here, I will summarize some aspects of these components, from the perspective of their observable radio emission. I will focus on the ionized jet itself and not in the entrained ambient gas that originates the molecular outflows. I will also focus on the dust component of the disk and not on the molecular component (e.g., see [20]), which may have an additional interest from the perspective of prebiotic chemistry.

2 Radio jets from young stellar objects

Jets are intrinsically associated with the star-formation process. They are collimated outflows, usually bipolar, that were first identified at visible wavelengths through the discovery of the systems of Herbig-Haro (HH) objects in the 1950's ([22], [21]). It was found the HH objects were moving away in opposite directions from a central position (the young star) with velocities of hundreds of km/s ([23]). Later-on, in the 1980's, with the advent of the new CCD detectors, weaker filamentary structures, apparently emerging from the central object and connecting it to the HH objects, were identified at the Calar Alto observatory ([29]) and were interpreted as jets. However, the observations at visible wavelengths have difficulties in reaching the region where the jet originates due to the increasing extinction in the proximity of the star. Observation of the radio continuum free-free emission of these sources does not have this handicap, making these "radio jets" a very useful tool to trace the base of the YSO jets at scales of 100 au or smaller (see [5], [7], [8]).

Radio jets are found in association with YSOs covering a wide range of stellar masses, from high to low mass protostars (Fig. 1), and possibly even in proto-brown dwarfs. Also, radio jets are found in all the phases of the star-formation process, from the extremely young protostars (Class 0 objects) to pre-main sequence stars (Class II-III objects) where accretion is very low (Fig. 2). In the different stages of the star-formation process, the results are consistent with a mass-loss rate of ∼10% of the mass accretion rate, suggesting a similar jet driving mechanism along all the stages of the star-formation process.

Unlike HII regions, radio jets are not photoionized, since they are found to be associated with low (and very low) luminosity stellar objects that lack the required ionizing photon rate to produce the observed radio luminosity ([4], [7]). Figure 3 shows the expected free-free radio continuum luminosity ($S_\nu d^2$) produced by potoionization (dot-dashed line) as a function of the bolometric luminosity of the object ($L_{\rm bol}$) and the observed data for very low luminosity (squares), low luminosity (dots) and high luminosity (triangles) objects. As can be seen in the figure, the observed radio emission of low and very low luminosity objects falls well above the values that photoionization can provide, indicating that it is not a feasible ionization mechanism. On the other hand, high luminosity objects fall below the values expected for photoionization, indicating that neither jets from low mass objects nor those from the massive ones are photoionized. Actually, the observed data points appear to follow the relationship $(S_\nu\, d^2\,/\,{\rm mJy~kpc}^2) = 0.008\,(L_{\rm bol}\,/\,L_\odot)^{0.6}$, which is valid over a wide range of bolometric luminosities, from 10^{-1} to 10^6 $L_\odot$. This correlation suggests that the same ionizing mechanism is at work in all kinds of radio jets, and provides a diagnostic tool to distinguish the radio emission of a photoionized HII region from that of a radio jet. This correlation also provides a way to predict the expected radio emission from embedded YSOs
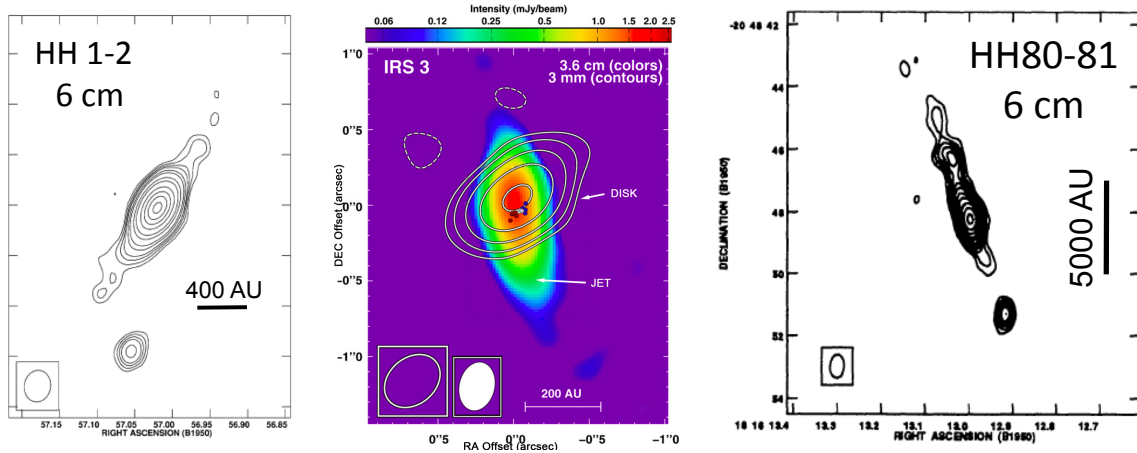
Figure 1: *Left:* Radio jet associated with the low-mass protostar driving the HH 1-2 system ([37]). *Left:* Disk-jet system associated with the intermediate-mass protostar IRS3 in NGC 2071 ([14]). Color scale indicates the free-free emission of the radio jet and contours indicate the dust emission of the disk. *Left:* Radio jet associated with the massive protostar driving HH 80 ([28]).
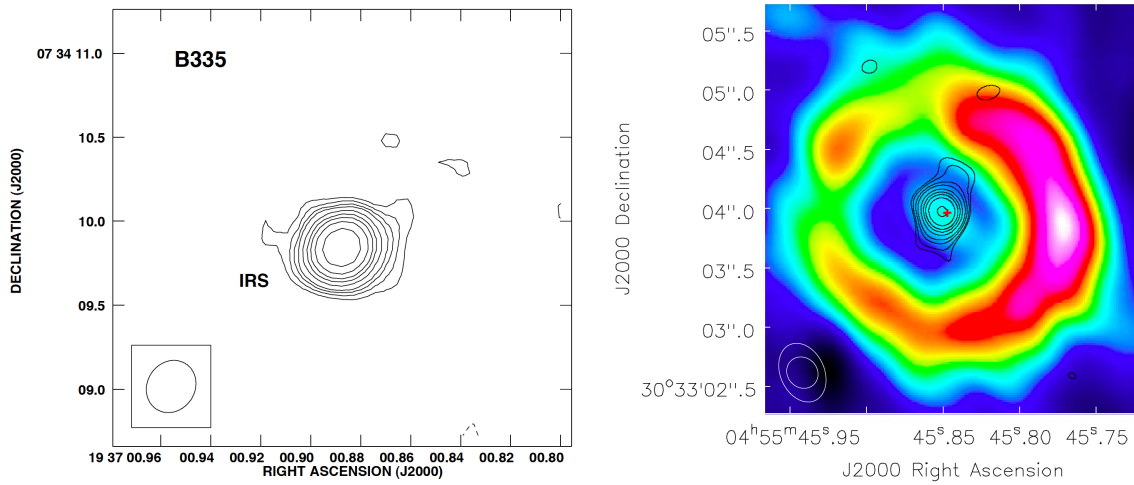

Figure 2: Radio jets (in contours) associated with the Class 0 protostar B335 (left; [36]) and with the pre-main sequence star AB Aur (right; [39]), which is associated with a transitional disk ([43]; in color scale).

of different luminosities (see [7]).

Since photoionization is discarded as the mechanism responsible for the ionization of radio jets, it was proposed that ionization by shocks associated with the jet itself could be a viable ionizing mechanism ([45], [17], [18]). Under this hypothesis, a relationship between the radio luminosity and the momentum rate of the outflow ($\dot{P}$) is expected ([5]). Figure 3 shows a
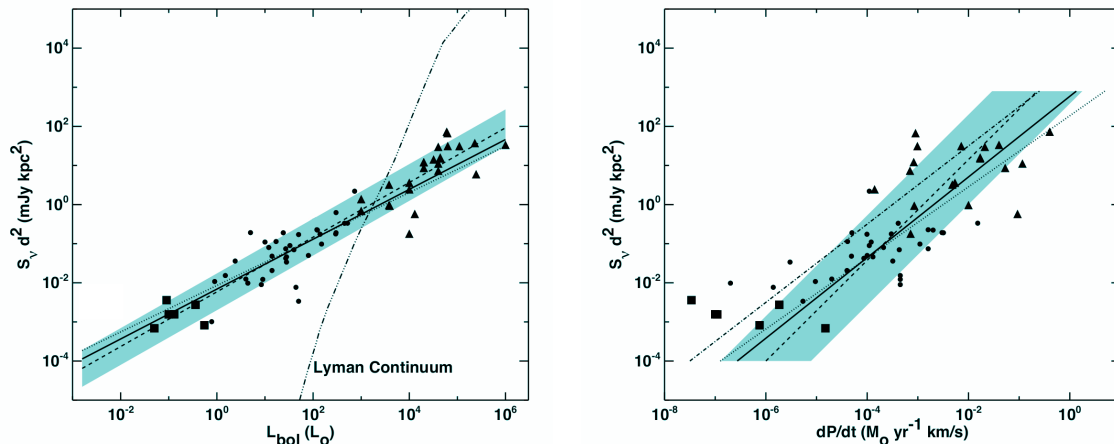
Figure 3: *Left:* Radio luminosity versus bolometric luminosity correlation for YSOs. Squares, dots, and triangles represent, respectively, very low, low, and high luminosity objects. The dashed line is a least-squares fit to all the data points and the grey area indicates the residual standard deviation of the fit. The solid line is a fit to the low-luminosity objects alone and the dotted line is the fit to the original sample of low-luminosity objects of [4]. The dot-dashed line (Lyman continuum) represents the radio luminosity expected from photoionization. *Right:* Radio luminosity versus outflow momentum rate (solid line). Symbols and line types of the fits are as in the left panel. The dot-dashed line is the maximum radio luminosity predicted by the shock ionization model of [17] and [18].

correlation between these two magnitudes, $(S_\nu\, d^2\,/\,\mathrm{mJy\,kpc^2}) = 190\,(\dot{P}\,/\,M_\odot\,\mathrm{yr^{-1}\,km\,s^{-1}})^{0.9}$, which is consistent with these expectations (see also [6], [5], [9], [7]). Therefore, shocks associated with the outflow itself are considered the likely mechanism for the ionization of radio jets. In summary, the radio luminosity at cm wavelengths is correlated with the bolometric luminosity of the YSO and the outflow momentum rate, providing a diagnostic tool to distinguish radio jets from other radio emitting objects.

Although radio jets from YSOs are characterized by thermal free-free emission, in a number of cases signs of non-thermal emission have been found in the jet lobes, at relatively large distances (several thousands of au) of the central object (e.g., [19], [28], [38], [40], [16] and references therein). The best studied case is the jet associated with HH 80, where linearly polarized emission has been maped, providing conclusive evidence for the presence of synchrotron emission in the jet ([15]; see Fig. 4). These observations give a direct measure of the magnetic field strength and distribution. However, measuring linear polarization in YSO jets is difficult because it is only a small fraction of the total emission and requires ultrasensitive observations.
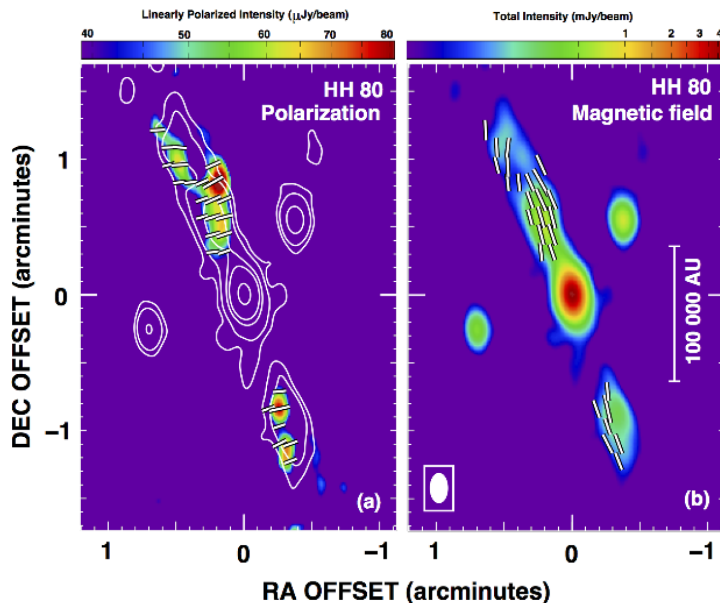
Figure 4: The HH 80 radio jet ([15]). The total intensity is shown in contours in the left panel and in color scale in the right panel, while the color scale in the left panel shows the linearly polarized intensity. The direction of the polarization and that of the magnetic field are shown as white bars in the left and right panels, respectively.

3   Protoplanetary disks and signs of planet formation

Circumstellar accretion disks of gas and dust are a natural output of the star-formation process. There is evidence that they are associated not only with low and intermediate mass stars but also with the massive ones ([33], [14]). These disks play a key role in the collimation of jets ([10]) and are the progenitors of planetary systems, although in the case of massive stars they are probably destroyed before the onset of planetary formation.

Some disks show evidence of central cavities devoid of dust, typically of tens of au in radius. These cavities were first inferred from the analysis of the spectral energy distribution (SED; [42], [11]) and more recently from direct imaging (right panel in Fig. 2 and Fig. 5). These cavities are considered signatures of the onset of planetary formation since they are attributed to the tidal effects of substellar objects or giant planets orbiting around the central star ([3], [31]). These disks are called transitional disks because it is believed that they are in transition between full disks that extend inward up tp very close distances to the star and those where most of the gas has been dissipated and a planetary system has been formed (see additional details in [30], [24]).

As the disk evolves, the dust grains grow in size, from submicron sizes (as in the interstellar medium) to mm-cm sizes in transitional disks, and finally reaching km sizes to form planetesimals and planetary bodies. Therefore, since the observed emission traces preferentially dust grains with sizes of the order of the observational wavelength, observations at
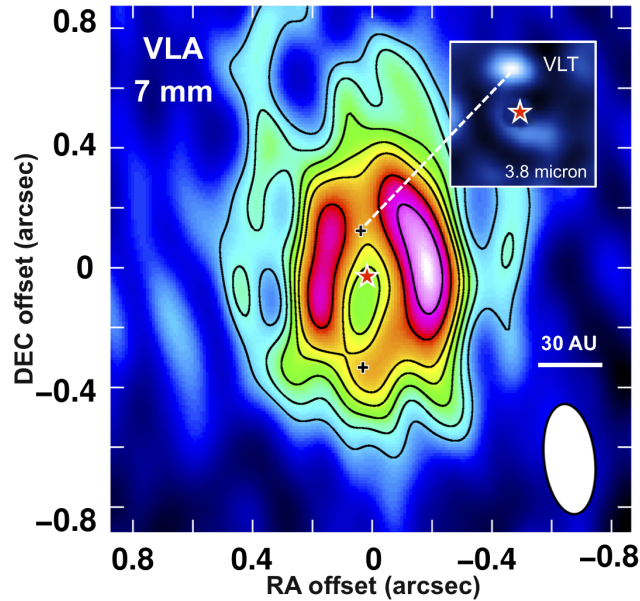
Figure 5:   *Top:* VLA image of the HD 169142 transitional disk at 7 mm ([31]). The inset in the upper-right corner shows, at the same scale, the infrared image at 3.8 μm of the protoplanet candidate inside the central cavity ([35]). *Bottom:* Sketch of the disk structure above the mid-plane ([31]).

mm/submm wavelengths are particularly well suited to study the dust emission of transitional disks. Indeed, the extremely sensitive and high angular resolution ALMA observations in this wavelength range have revolutionized the study of these objects, revealing central cavities, spiral arms, dust traps, and other features associated with the early stages of planetary formation ([46], [44]). Particularly intriguing are the results of the highest angular resolution images ($\sim 0.03''$), such as the ringed substructure with multiple gaps observed in the HL Tau disk, even when this object is believed to be in an early stage, prior to the development of a transitional disk ([2]); or the dwarf, probably transitional, disk imaged in XZ Tau B ([32]; see [30]). These observations have revealed, also, that at small radii the emission can be optically thick, even at mm wavelengths. In this respect, observations at longer wavelengths, where the emission is optically thin, can provide improved information, as shown by the VLA

results at 7 mm in HL Tau, that reveal hints of fragmentation in the inner ring of HL Tau ([13]; see Fig. 6).
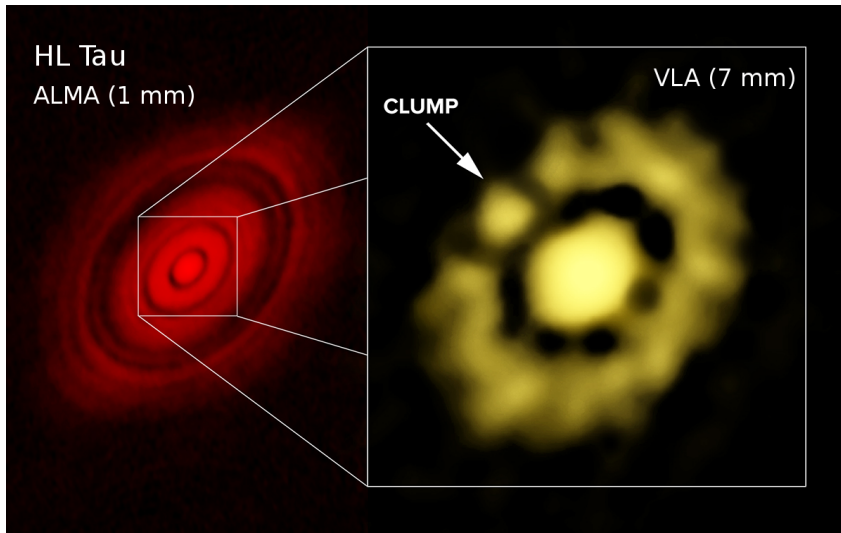

Figure 6: *Left:* ALMA image of the HL Tau disk at 1 mm ([2]). *Right:* VLA image at 7 mm of the inner ring (radius = 20 au), showing signs of fragmentation ([13]).

Observations at cm wavelengths are also better suited to study more advanced phases of the disk evolution, where dust grains have reached the pebble size. However, at cm wavelengths the free-free emission of the jet may be dominant and it is necessary to properly separate the emissions of dust and ionized gas through a good knowledge of the SED and using high resolution images that allow a separation of the different components. The last stages of disk evolution should be characterized by the dispersal of the gas component. Photoevaporation of the disk by high energy radiation is considered the dominant mechanism for gas removal ([1]). In this respect, [27] have recently obtained direct evidence for this mechanism being at work in GM Aur by spatially separating and imaging with the VLA at 3 cm wavelength the dust emission of the disk, the ionized jet, and the ionized photoevaporating disk (see Fig. 7). In this source, at 7 mm $\sim 85\%$ of the emission corresponds to dust and $\sim 15\%$ corresponds to free-free, while at 3 cm only $\sim 15\%$ corresponds to dust and $\sim 50\%$ of the remaining free-free emission corresponds to the jet and $\sim 35\%$ to the photoevaporating disk.

4   Prospects for the Square Kilometre Array

The results already obtained with the VLA at 7 mm and longer wavelengths anticipate some of the expected achievements for a high angular resolution, high sensitivity facility such as the SKA. SKA will be able, even in its Phase 1, to make a deep survey of YSO radio jets in the southern hemisphere. It will detect and accurately trace the position of deeply embedded YSOs. As estimated from the correlations discussed in section 2 and shown in Figure 3, it is
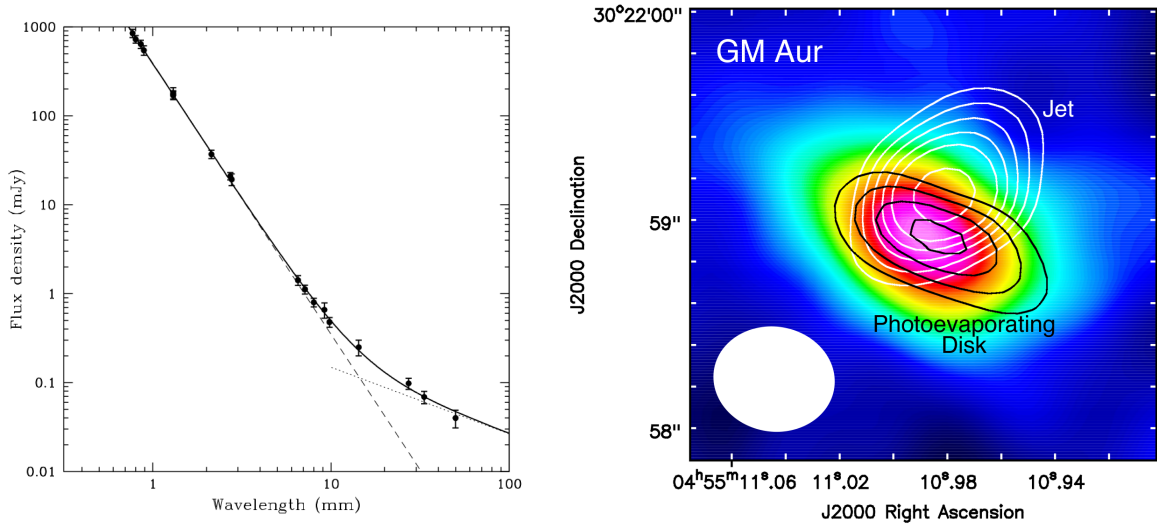
Figure 7: *Left:* SED of GM Aur in the mm-cm wavelength range, showing the contributions of the dust and free-free components. *Right:* VLA image of GM Aur showing the dust emission of the disk at 7 mm, the ionized jet at 3 cm and the ionized photoevaporating wind at 3 cm (both figures are from [27]).

expected that SKA will be able to detect all proto-brown dwarfs within 500 pc and all the massive protostars in the Galaxy.

Detailed studies of relatively strong jets at very high angular resolution could be undertaken in order to determine the variation of physical parameters along the jet axis, to image the region around the injection radius of the ionized gas, and to efficiently separate the free-free emission of the jet from the dust emission of the disk.

So far, only the radio continuum emission of the ionized jets has been detected since radio recombination lines fall below the sensitivity limits of the current instrumentation (with the exception of sources with maser amplification; [25]). SKA Phase 1 will be able to detect the radio recombination lines in radio jets providing the radial component of the velocity that, together with proper motions measurements (that are already feasible), will give the full 3D kinematics of these objects.

SKA will be able to map the linear polarization and magnetic field in radio jets with bright knots (Phase 1) and in an extended sample of jets with the full SKA. This information, when combined with the remaining physical parameters inferred from the thermal emission will provide a full characterization of YSO jets, that will give key information to understand all astrophysical jets.

SKA will provide images of the distribution of large (several cm) dust grains and pebbles in protoplanetary disks. This emission is expected to be optically thin essentially over all the disk structure, allowing to study the grain grow process, dust migration, and trapping associated with planet formation.

SKA is expected to image and characterize the properties of the photoevaporative winds

in nearby protoplanetary disks, in order to study the gas dispersal mechanisms.

Acknowledgments

References

[1] Alexander, R., Pascucci, I., Andrews, S., Armitage, P., & Cieza, L. 2014, Protostars and Planets VI, 475

[2] ALMA Partnership, Brogan, C. L., Pérez, L. M., et al. 2015, ApJL, 808, L3

[3] Andrews, S. M., Wilner, D. J., Espaillat, C., et al. 2011, ApJ, 732, 42

[4] Anglada, G. 1995, RevMexAA Conf. Ser., 1, 67

[5] Anglada, G. 1996, Radio Emission from the Stars and the Sun, ASP Conf. Ser., 93, 3

[6] Anglada, G., Rodríguez, L. F., Cantó et al. 1992, ApJ, 395, 494

[7] Anglada, G., Rodríguez, L.F., & Carrasco-González, C. 2015, Advancing Astrophysics with the Square Kilometre Array (AASKA14), 121

[8] Anglada, G., Tafalla, M., Carrasco-González, C., et al. 2015, in The Spanish Square Kilometre Array White Book, eds. M. Pérez-Torres et al., p. 169

[9] Anglada, G., Villuendas, E., Estalella, R., et al. 1998, AJ, 116, 2953

[10] Blandford, R. D., & Payne, D. G. 1982, MNRAS, 199, 883

[11] Calvet, N., D'Alessio, P., Watson, D. M., et al. 2005, ApJL, 630, L185

[12] Carrasco-González, C., Galván-Madrid, R., Anglada, G., et al. 2012b, ApJL, 752, L29

[13] Carrasco-González, C., Henning, T., Chandler, C. J., et al. 2016, ApJL, 821, L16

[14] Carrasco-González, C., Osorio, M., Anglada, G., et al. 2012a, ApJ, 746, 71

[15] Carrasco-González, C., Rodríguez, L. F., Anglada, G., et al. 2010, Science, 330, 1209

[16] Carrasco-González, C., Rodríguez, L. F., Anglada, G., et al. 2013, European Physical Journal Web of Conferences, 61, 03003

[17] Curiel, S., Canto, J., Rodriguez, L. F. 1987, RevMexAA, 14, 595

[18] Curiel, S., Rodriguez, L. F., Bohigas, J., Roth, M., Canto, J., Torrelles, J. M. 1989, Astrophys. Lett. Comm., 27, 299

[19] Curiel, S., Rodríguez, L. F., Moran, J. M., et al. 1993, ApJ, 415, 191

[20] Fuente, A., Agúndez, M., Cernicharo, J. et al. 2016, this volume

[21] Haro, G. 1952, ApJ, 115, 572

[22] Herbig, G. H. 1951, ApJ, 113, 697

[23] Herbig, G. H., & Jones, B. F. 1981, AJ, 86, 1232

[24] Huélamo, N. 2016, this volume

[25] Jiménez-Serra, I., Martín-Pintado, J., Báez-Rubio, A., Patel, N., & Thum, C. 2011, ApJL, 732, L27

[26] Macías, E. 2016, PhD Thesis, University of Granada

[27] Macías, E., Anglada, G., Osorio, M. et al., 2016, ApJ 829, 1

[28] Martí, J., Rodríguez, L. F., & Reipurth, B. 1993, ApJ, 416, 208

[29] Mundt, R., & Fried, J. W. 1983, ApJ, 274, L83

[30] Osorio, M. 2016, this volume

[31] Osorio, M., Anglada, G., Carrasco-González, C., et al. 2014, ApJL, 791, L36

[32] Osorio, M., Macías, E., Anglada, G., et al. 2016, ApJL, 825, L10

[33] Patel, N. A., Curiel, S., Sridharan, T. K., et al. 2005, Nature, 437, 109

[34] Pudritz, R. E., & Norman, C. A. 1983, ApJ, 274, 677

[35] Reggiani, M., Quanz, S. P., Meyer, M. R., et al. 2014, ApJL, 792, L23

[36] Reipurth, B., Rodríguez, L. F., Anglada, G., & Bally, J. 2002, AJ, 124, 1045

[37] Rodríguez, L. F., Delgado-Arellano, V. G., Gómez, Y., et al. 2000, AJ, 119, 882

[38] Rodríguez, L. F., Garay, G., Brooks, K. J., et al. 2005, ApJ, 626, 953

[39] Rodríguez, L. F., Zapata, L. A., Dzib, S. A., et al. 2014, ApJL, 793, L21

[40] Rodríguez-Kamenetzky, A., Carrasco-González, C., Araudo, A., et al. 2016, ApJ, 818, 27

[41] Shu, F. H., Adams, F. C., & Lizano, S. 1987, ARA&A, 25, 23

[42] Strom, K. M., Strom, S. E., Edwards, S., Cabrit, S., & Skrutskie, M. F. 1989, AJ, 97, 1451

[43] Tang, Y.-W., Guilloteau, S., Piétu, V., et al. 2012, A&A, 547, A84

[44] Tobin, J. J., Kratter, K. M., Persson, M. V., et al. 2016, Nature, 538, 483

[45] Torrelles, J. M., Ho, P. T. P., Rodriguez, L. F., Canto, J. 1985, ApJ, 288, 595

[46] van der Marel, N., van Dishoeck, E. F., Bruderer, S., et al. 2013, Science, 340, 1199